UFSM

CIÊNCIA e NATURA

ISSN 2179-460X
Acesso aberto

Ci. e Nat., Santa Maria, v. 43, e73, 2021 • https://doi.org/10.5902/2179460X64223
Submitted: 01/04/2021 • Approved: 19/07/2021 • Published: 31/12/2021

Environment

Adsorption of remazol golden yellow dye from aqueous solution by acerola core: kinetic and equilibrium studies

Adsorção do corante remazol amarelo ouro de solução aquosa por caroço de acerola: estudos cinéticos e de equilíbrio.

Ada Azevedo Barbosa[I], Marina Gomes Silva[I], Ingrid Larissa da Silva Santana[I], Ramon Vinícius Santos de Aquino[I], Naiana Santos da Cruz Santana Neves[I], Isis Henriqueta dos Reis Ferreira[I], Otidene Rossiter Sá da Rocha[I]

[I]Universidade Federal de Pernambuco, Recife, PE, Brazil

ABSTRACT

This work was conducted to evaluate the efficiency of the acerola (*Malpighia emarginata*) core as adsorbent (ACB) and as a precursor of adsorbent charcoal (CAB) and activated charcoal (ACP), to remove the textile dye remazol golden yellow (RGY) in solution. The adsorbents characterization was obtained by Fourier-transform infrared spectroscopy, thermogravimetric analysis (TG) and determination of the specific area and the point of zero charge (pHpzc). The best conditions for adsorption for this adsorbent was reached through adsorbent mass studies and kinetic and equilibrium assays. The adsorption capacity q ($mg.g^{-1}$) was used to analyze the effects. The pHpzc were 4.15 for ACB, 6.00 for CAB and 4.32 for ACP, demonstrating superficial charge favorable to dye adsorption. Considering the kinetic aspects, the pseudo-first order model adjusted more satisfactorily to experimental data. Related to isotherms, Langmuir was more efficient to represent experimental data of dye adsorption. ACB, CAB and ACP are potential adsorbents for dyes in effluents, presenting maximum adsorption capacity, in the study conditions, of 52.35 $mg.g^{-1}$, 16.40 $mg.g^{-1}$, and 119.00 $mg.g^{-1}$, respectively.

Keywords: Acerola core; Biosorption; Remazol golden yellow; Textile wastewater

RESUMO

Neste trabalho, foi avaliada a eficiência de caroços de acerola (Malpighia emarginata) como adsorvente (ACB) e precursor de carvão (CAB) e carvão ativado (ACP) para a remoção do corante têxtil remazol amarelo ouro (RGY) em solução. A caracterização dos adsorventes foi feita por espectroscopia de infravermelho por transformada de Fourier, análise termogravimétrica (TG) e determinação da área específica e do ponto de carga zero (pHpzc). As melhores condições de adsorção para esses adsorventes

foram alcançadas após estudos de massa de adsorvente e testes cinéticos e de equilíbrio. A capacidade adsortiva q ($mg.g^{-1}$) foi utilizada para verificar a eficiência de adsorção. Os valores de pHpzc foram de 4,15 para ACB, 6,00 para CAB e 4,32 para ACP, mostrando uma carga superficial favorável para a adsorção do corante. Considerando a cinética, o modelo de pseudo-primeira ordem ajustou-se satisfatoriamente aos dados experimentais. Em relação às isotermas, o modelo de Langmuir foi mais eficiente para representar os dados experimentais. ACB, CAB e ACP são potenciais adsorventes para corantes em efluentes, apresentando capacidade de adsorção máxima, nas condições desse estudo, de 52,35 $mg.g^{-1}$, 16,40 $mg.g^{-1}$ e 119,00 $mg.g^{-1}$, respectivamente.

Palavras-chave: Biossorção; Caroços de acerola; Efluentes Têxteis; Remazol amarelo ouro

1 INTRODUCTION

Pollution and environment destruction, as a result of industrialization, have been a serious current problem, because of the large amount of effluents generated by industries of different branches such as tannery, textile, pharmaceutical, food, paper and cellulose, petrochemical along with others. Each industrial process presents difficulty to reach the acceptable limits, established by the current law, due to the complex composition of the pollute (ARAUJO et al. 2014; AZIZ et al. 2016; BARBOSA et al. 2019).

The textile sector frequently related to negative environmental impacts related to industrial effluents, because of the large amount of dyes used in the tannery process. The discharge of wastewater with color harms the aquatic habitat, changing its color and creating conditions to eutrophication, low oxygenation and reduction of sunlight penetration (HASSAAN et al. 2017; HOLKAR et al. 2016; JARAMILLO-SIERRA et al. 2019).

Among the most used techniques for dye removal in wastewater are coagulation/flocculation, photodegradation, filtration, solvent extraction, adsorption by activated carbon and biological treatment (BARBOSA et al. 2019; CHAKMA et al. 2015; LI et al. 2016; WAWRZKIEWICZ et al. 2015). Each method presents pro and cons, and for its choice, there are some parameters that must be considered: efficiency, safety, simplicity, sludge formation, construction and operation costs, required space and impact in the receptor medium.

Conventional methods are not always convenient or completely efficient and can even have high costs (BHATNAGAR; SILLANPÄÄ, 2010). Therefore, it is necessary to develop and implement treatment technologies that are environmentally friendly, sustainable, efficient energetically and economically viable.

Amidst processes, adsorption stands out because of the insensibility for toxic substances, simplicity in its project and operation, easy recovery and low costs (ANGIN, 2014). Diverse adsorbent materials have been used in adsorption processes. The activated carbon is the most used material due to its adsorption capacity and the versatility of different precursors in its production. The raw materials normally used are mineral charcoal, wood, turf, petroleum waste, animal bones and others.

Some biomasses have already been evaluated as adsorbents for dye removal, such as agave (SÁNCHEZ-NAVA et al. 2019), orange peel (AHMED et al. 2020), pomelo peel (ZHANG et al. 2020), banana peel (HASHEM et al. 2020), garlic peel (ZHAO et al. 2020), potato peel (BOUHADJRA et al. 2021) and fava bean peel (BAYOMIE et al. 2020). In this way, the solid waste becomes a great option to substitute the commercial activated carbon due to its availability in the agroindustrial sector.

Finally, this work proposed to evaluate the use of adsorbents prepared from the agroindustrial waste acerola (Malpighia emarginata) core, for adsorption of the dye remazol golden yellow (RGY) in aqueous solution, aiming the application in treatment processes of textile industries effluent.

2 MATERIALS AND METHODS

2.1 Dye solution preparation

For the stock solution (400 mg.L^{-1}) preparation, 400mg of dye remazol golden yellow RNL ($C_{16}H_{18}N_4O_{10}S_3Na_2$, pKa = 3.0, 3.5 and 6.0 for sulphonic groups) were weighed out on analytical balance and dissolved in 1 liter of water. The subsequent solutions were prepared by the dilution of the stock one. The structure of RGY is presented in Figure 1.

Figure 1 - Remazol Golden Yellow RNL structure

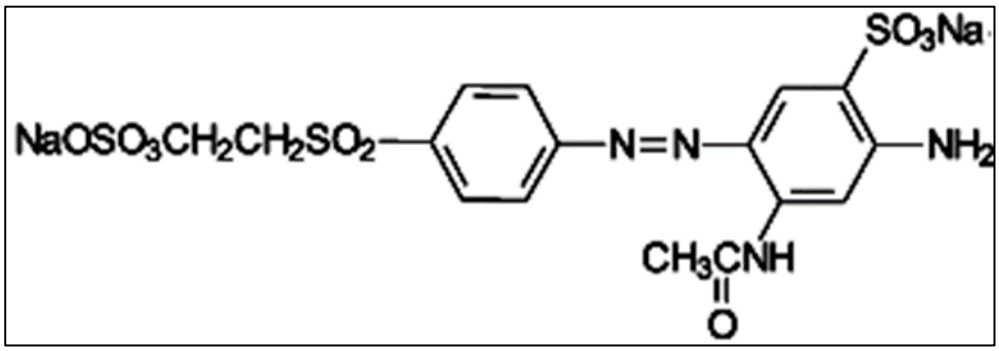

Source: Authors (2021)

In order to determine the wavelength of the point of maximum adsorbance of the dye, it was realized a scanning by UV-Visible spectrometer (Thermo Scientific, model Genesys 10S) through the range from 190 to 800 nm. The analytical curve was produced in the range from 0.1 to 100 mg.L^{-1}.

2.2 Preparation of the precursor material and adsorbents

To obtain the precursor adsorbent (ACB), the agroindustrial waste was crushed in a semi industrial food processor, dried at 110 ºC for 24 hours in oven (Marconi MA035/1), milled in knife mill (TECNAL) to particles with size of 212 mm/Um, and, finally, sieved through a 65 mesh sieve.

For the purpose of attaining the carbonized adsorbent (CAB), the dried acerola bran was heated in a muffle (Vulcan 3-550) during 60 minutes at 200 ºC, and later on 20 minutes at 250 ºC, with heating rate of 5 ºC.min^{-1}.

The activated carbon adsorbent (ACP) was developed by previous chemical treatment. The dried acerola bran was impregnated with phosphoric acid (F. Maia, 85%) (1g of agent: 1g of precursor) and heated to 80 ºC, under manual stirring by approximately 30 minutes. Next, it was dried by oven at 110 ºC by 24 hours. The carbonization of the material was carried out in a muffle (Vulcan 3-550) during 60 minutes at 200 ºC and 20 minutes at 250 ºC, with heating rate of 5 ºC.min^{-1}. The obtained carbon was immersed in a solution of hydrochloric acid (Qhemis, 37%) by 20 minutes and washed with distillated water until the neutral pH was reached. After, the material was dried in oven at 80 ºC by 8 hours and stored in a recipient hermetically sealed. According to the stage of processing, the prepared materials were codified in Table 1.

Table 1 - Codification of samples obtained during the activated carbon synthesis

Code	Material
ACB	Raw acerola (*Malpighia emarginata*) core bran
CAB	Carbonized acerola core bran
ACP	Acerola core charcoal activated with H_3PO_4

Source: Authors (2021)

2.3 Adsorbent Characterization

The Fourier-transform infrared spectroscopy analysis (FTIR) was used to verify the organic compounds of the adsorbents. The analyses were carried out in the range from 4000 to 500 cm^{-1}with a spectrometer (Bruker tensor 27) with a detector DLaTGS and a probe ATR (attenuated total reflectance). The spectrums were presented in spectral resolution of 4 cm^{-1} and average of 128 scans, in room temperature (23 ± 2°C).

The evaluation of mass loss in the adsorbent samples was realized by thermogravimetric analysis. Hence, it was carried out temperature variations from

25 to 900°C, using 10mg of precursor, in alumina crucible in an equipment Perkin Elmer STA 6000 with simultaneous thermic analysis (TGA). The texture characterization by Brunauer, Emmett and Teller method (BET) was used to determine the superficial area (SBET), volume and medium size of the pores of the adsorbents in an equipment Quanta Chrome (model NOVA) by physisorption (adsorption/ desorption of N_2 at 77 K).

2.4 Point of zero charge determination

The pH of the point of zero charge (pHpzc), for the studied adsorbents, was determined by measurements of the water pH before and after the contact with the solids according to Schimmel *et al.* (2010). An amount of 0.1 g of the adsorbents was added in 25 mL of water with pH varying from 2 to 10 adjusted in pHmeter (Tecnal, TEC-2). For the adjustment were used solutions of hydrochloric acid 0.1 $mol.L^{-1}$(from Química Moderna) and sodium hydroxide 0.1 $mol.L^{-1}$(from Dinâmica). The solutions were stirred in shaker table (IKA, KS 130 control) at 200 rpm for 24 hours. The pHpzc was detected through the graphic of (pHfinal–pHinitial) vs. pHinitial, corresponding to the range where the final pH is constant independently of the initial pH, that is, the surface behaves as a buffer solution.

2.5 Influencer of initial pH of the dye solution

The effect of the initial pH of the RGY solution (100 $mg.L^{-1}$) was investigated from pH 2 to 10. The studied adsorbents (0.1 g) were added in 25 mL of the dye solutions in the range of pH and stood under agitation at 200 rpm for 6 hours.

2.6 Influence of adsorbent amount

Assays were performed to evaluate the adsorbent concentration in order to compare the removal percentage and adsorption capacity. The adsorbent

concentration effect was studied in the range from 4 to 40 $g.L^{-1}$and the tests used 25mL of RGY solution (100 $mg.L^{-1}$) under agitation of 300 rpm for 6 hours, according to Silva (2015), and the pH defined in the preceding study. The calculus of the amount adsorbed by the adsorbent mass was obtained from Equation 1.

$$q_e = \frac{(C_0 - C_f)V}{m} \quad (1)$$

Where, q_e is the adsorption capacity ($mg.g^{-1}$); C_o, the initial dye concentration ($mg.L^{-1}$); C_f, the final dye concentration ($mg.L^{-1}$); V, the solution volume (L) and m, the adsorbent mass (g). The reached results of adsorption capacities were assessed in the kinetic and equilibrium studies.

2.7 Kinetic and Adsorption Equilibrium Studies

Kinetic and adsorption equilibrium studies were performed by contacting the adsorbents with the RGY solutions of concentration of 10, 20, 40, 60 and 100 $mg.L^{-1}$. For each isotherm, times from 0 to 360 minutes were evaluated. The adsorption isotherms were obtained from the addition of 0.062; 0.175 and 0.043g of the adsorbents raw (ACB), carbonized (CAB) and activated (ACP), respectively, in 25 mL of the dye solution. The adsorbents masses were determined in the mass study.

The Table 2 presents the mathematic models that were used for the kinetic and equilibrium study. The kinetic models of pseudo-first order, pseudo-second order and Elovich were used to adjust the experimental data. The first two were chosen because they are the most widely used in adsorption kinetics, whereas the third is complementary and can provide evidence of chemical adsorption. To evaluate the equilibrium, the adsorption models of Langmuir, Freundlich and Fritz Schlunder were applied. Langmuir and Freundlich are the most usual models for equilibrium isotherms, while Fritz Schlunder is a three-parameter model that

combines features of the first two models. The mathematic models were adjusted to experimental data by a non-linear regression method (Origin 8.0).

Table 2 - Mathematic models adjusted to experimental data in the kinetic and equilibrium studies

Models	Kinetics	Equations	
Kinetic	Pseudo-first order	$\frac{dq_t}{d_t} = k_1(q_e - q_t)$	(2)
	Pseudo-second order	$\frac{dq_t}{d_t} = k_2(q_e - q_t)^2$	(3)
	Elovich	$\frac{dq_t}{d_t} = \alpha \exp(-\beta q_t)$	(4)
Equilibrium	Langmuir	$q_e = K_F C_e^{1/n}$	(5)
	Freundlich	$q_e = \frac{q_{max} k_L C_e}{1 + k_L C_e}$	(6)
	Fritz Schlunder	$q_e = \frac{k_{FS} C_e^{b1}}{1 + a C_e^{b2}}$	(7)

Source: Authors (2021)

Where k_1, the pseudo-first order adsorption rate constant (min^{-1}), *qe*, the adsorption capacity in the equilibrium, *qt*, the adsorption capacity through time ($mg.g^{-1}$); t, time (minutes), k_2, the pseudo-second order adsorption rate constant ($gmg^{-1}.min^{-1}$);α, the initial adsorption rate ($mg.g^{-1}\ min^{-1}$) and β is the desorption constant ($g.mg^{-1}$).C_e is the dye concentration in the equilibrium ($mg.L^{-1}$), qmax, the maximum capacity of dye sorption ($mg.g^{-1}$) and k_L the Langmuir constant for equilibrium adsorption, which demonstrates the affinity level between adsorbent and adsorbate ($L.mg^{-1}$). K_F expresses in a constant the adsorption capacity of the adsorbent ($mg.g^{-1}$).($mg.L^{-1}$) and *1/n* is the dimensionless term that represents the adsorption intensity. KFS expresses the constant of Fritz-Schlunder, and b1 and b2, the heterogeneity factors.

The model parameters were obtained by the minimization of the sum of the minimum square deviations among the experimental and predict values. The model adjustment was evaluated through the calculus of the relative standard deviations (σ_i) and the regression coefficients (R^2). The performance of the best adjusted models was compared by the test F (MONTGOMERY, 2012). F_{cal} was calculated from the equation 8.

$$F_{cal} = \frac{S_R^2(A)}{S_R^2(B)} \quad (8)$$

Where SR (A) and SR (B) are respectively the deviations of models A and B, for SR(A) > SR(B). If $F_{cal} > F_{tabulated}$, the model B presents an adjustment better than the model A in a 95% confidence level.

3 RESULTS AND DISCUSSION

3.1 Adsorbent Characterization

The Fourier-transform infrared spectroscopy analysis (FTIR) was conducted in the wavenumber range from 500 to 4000 cm^{-1}. Figure 2 presents the spectrums with the identification of the adsorption chemical groups.

Figure 2 - FTIR of adsorbents raw (ACB), carbonized (CAB) and activated (ACA)

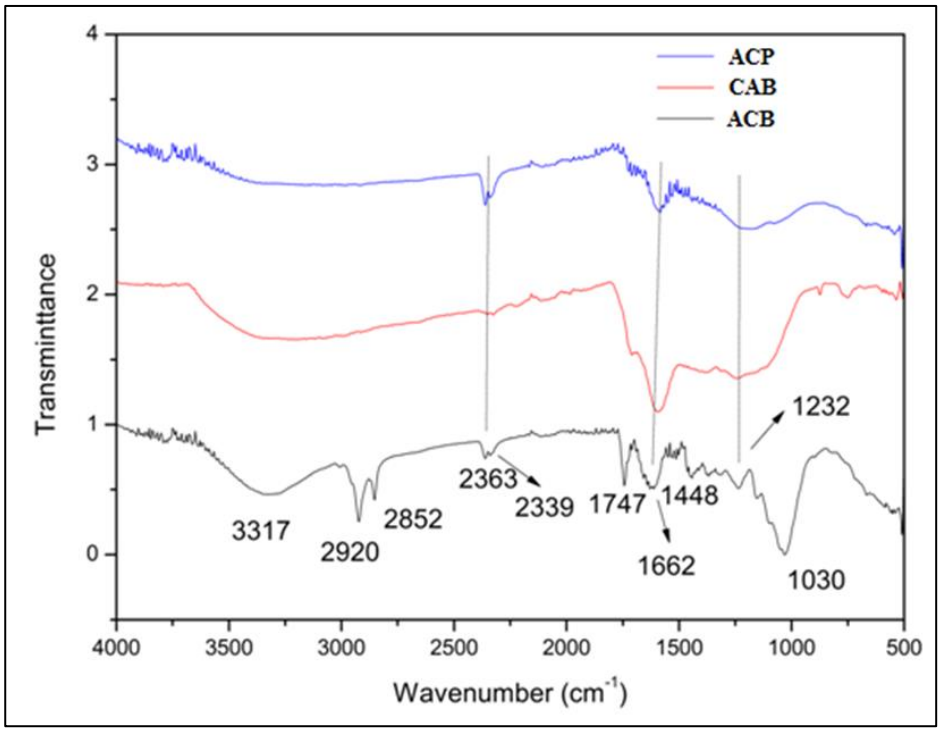

Source: Authors (2021)

In Figure 2, a band is observed in the range3281-3348 cm^{-1}, which represents a stretching of the group O-H (SOLOMONS; FRYHLE, 2012; TOMUL *et al.* 2019). This band reduces its intensity whilst the precursor goes through carbonization and activation. The same effect happens with the bands 3012, 2920 and 2852 cm^{-1} and are related to the groups –CH, -CH_3 and –CH_2 respectively, possibly due to the presence of hemicellulose, cellulose and lignin (SILVERSTEIN *et al.* 2006), that are degraded by the use of temperature and by the activation agent H_3PO_4. In 2363 and 2339 cm^{-1}, the characteristic band of disubstituted alkynes (C≡C) is observed (TRAN; CHAO, 2018). In this case, after the carbonization process, it was not possible to verify the presence of this group.

The stretching vibration of the group carboxyl is represented at 1747 cm^{-1}, with intensity peak for the natural adsorbent (ACB). While the precursor went through each treatment, this band diminished its intensity. The bands at 1662 and 1448 cm^{-1} correspond to the aromatic group C=C (REDDY *et al.* 2011). It was observed that for the band at 1662 cm^{-1} there was an intensity reduction for the

chemical treatment, whilst for the band at 1448 cm^{-1} there was an intensity reduction even for the thermal treatment, reducing still more in the activation process. The possible presence of lignin can be still verified by the bands 1030, 1151 and 1232 cm^{-1} that correspond to the stretching C-O of alcohols and phenol (VIOTTI *et al.* 2019) and presented the bands 3012, 2920 and 2852 cm^{-1} for the three adsorbents.

The Table 3 demonstrates the values of superficial area, volume and pore diameter related to each type of adsorbent.

Table 3 - Textural characterization of the adsorbents

	Superficial Area ($m^2.g^{-1}$)	**Pore Volume ($cm^3.g^{-1}$)**	**Pore Diameter (nm)**
ACB	-	0.0354	4.463
FAP	23.63	0.00287	3.964
ACP	375.90	0.01347	3.598

Source: Authors (2021)

According to the data in Table 3, the adsorbent ACP presented the greater superficial area (375.90 $m^2.g^{-1}$). This can be explained by the utilization of a dehydrating agent H_3PO_4 for the activation. Moreover, the superficial area gain causes the reduction of pore size. Therefore, the raw adsorbent featured the greater volume and pore diameter.

The thermogravimetric analysis allowed evaluating the behavior of the adsorbents when submitted to temperature variations from 25 to 900 ºC, as reported by Figure 3.

According to Figure 3, the natural adsorbent demonstrated a mass loss more accentuated than the other adsorbents, with 83% of loss. This is related to the treatment method that does not use high temperature in its preparation. Comparing the carbonized adsorbent and the carbonized and activated one, it is observed that the utilization of the activating agent did not cause significant

difference in mass loss, once they presented final loss of 57.6% and 59.5%, respectively.

Figure 3 - Thermogravimetric curve of adsorbent (a) natural (ACB), (b) carbonized (CAB) and (c) activated (ACP)

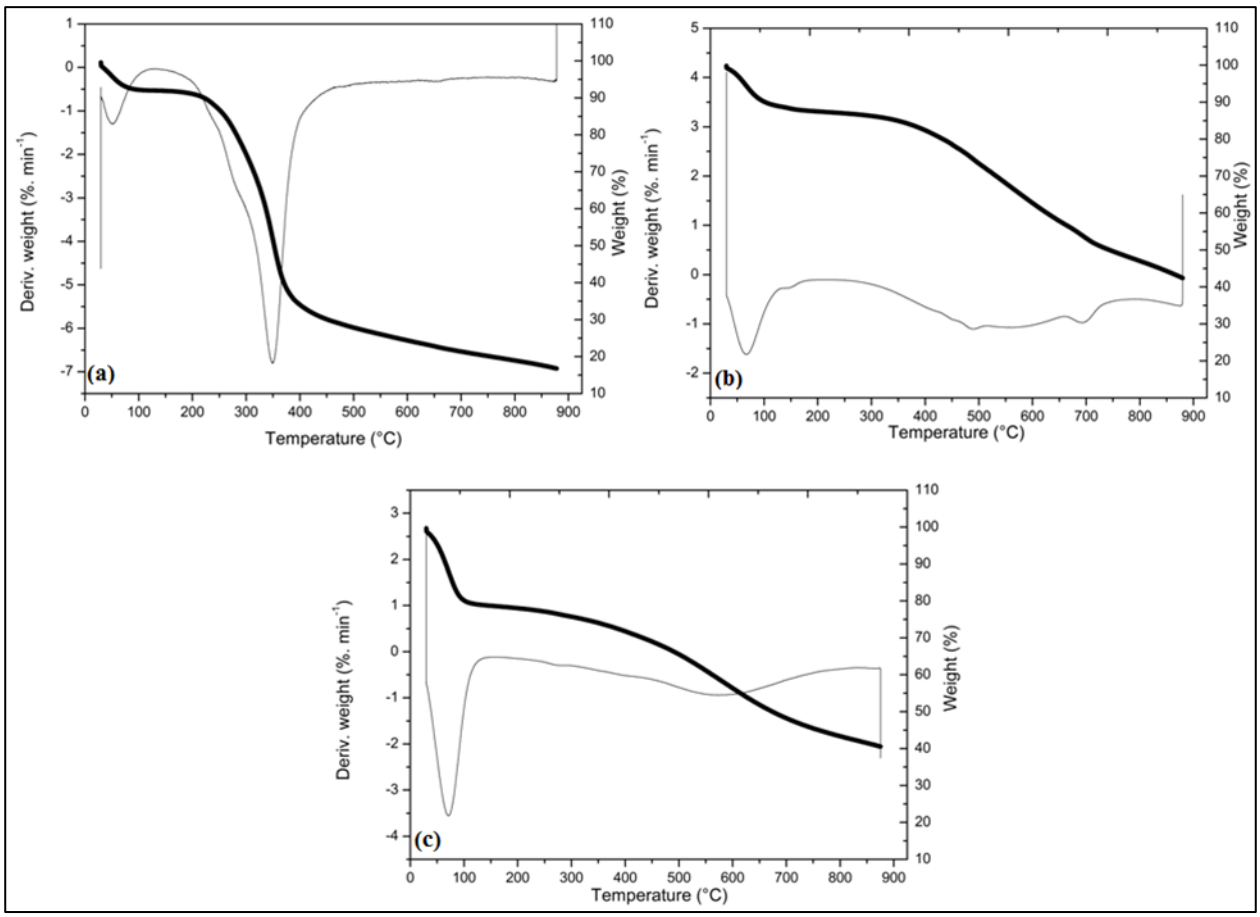

Source: Authors (2021)

3.2 Point of zero charge determination

The point of zero charge is an important parameter because it provides information about the charges behavior on the adsorbent surface as a function of the medium pH. In Figure 4, the point of zero charge is represented for the determination of the superficial charge of the adsorbents ACB, CAB, ACP.

As stated in Figure 4, the curve intersection with the horizontal axis ($pH_{initial}$ scale) occurred at pH 4.15 for the raw acerola core bran (ACB), 6.0 for the carbonized acerola core bran (CAB) and 4.42 for the charcoal of acerola core

activated with H_3PO_4 (ACP). As reported by Tagliaferro *et al.* (2011) the anion adsorption is facilitated at a pH lower than the pHpzc, because, in this case, the liquid charge of the adsorbent surface is positive, whereas the cation adsorption is promoted at a pH higher than pHpzc, once the liquid charge of the adsorbent surface is negative.

Figure 4 - Point of zero charge (pHpzc). Experimental conditions: pH 2 to 10, agitation speed = 300 rpm, t = 24h

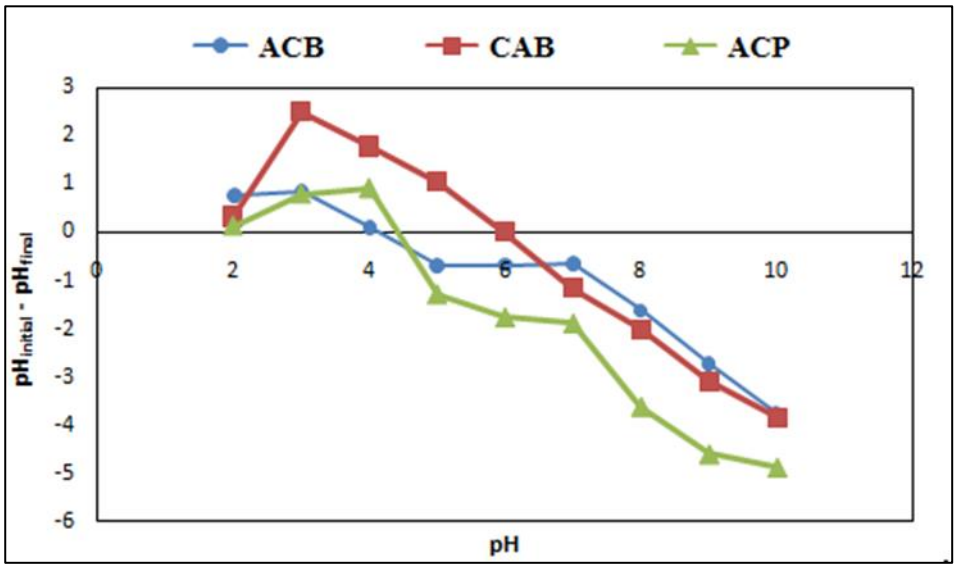

Source: Authors (2021)

3.3 Influence os initial pH of thw dye solution

Dye aqueous solutions can behave in different manners regarding to an adsorbent material when the solution pH is varied. Thus, the pH change can activate or deactivate the present active sites, causing alteration in the adsorption capacity, and, consequently, in the removal percentage of contaminants, in this case, the RGY solution. Figure 5 shows the adsorption capacity of the studied adsorbents (ACB, CAB, ACP) related to different pH of RGY solutions.

In consonance with the Figure 5, the adsorbents ACB, CAB and ACP presented greater adsorption capacity at pH 2. This result was expected considering that the adsorbents have basic character. The adsorption process was facilitated for the

solution with acidic pH because, in this case, there was a greater interaction between the adsorbent and adsorbate, due to the difference of positive and negative charges.

Figure 5 - Influence of initial pH of RGY solution. Experimental conditions: pH 2 to 10, C0= 50 mg.L^{-1}; agitation speed = 300 rpm, t= 360 min

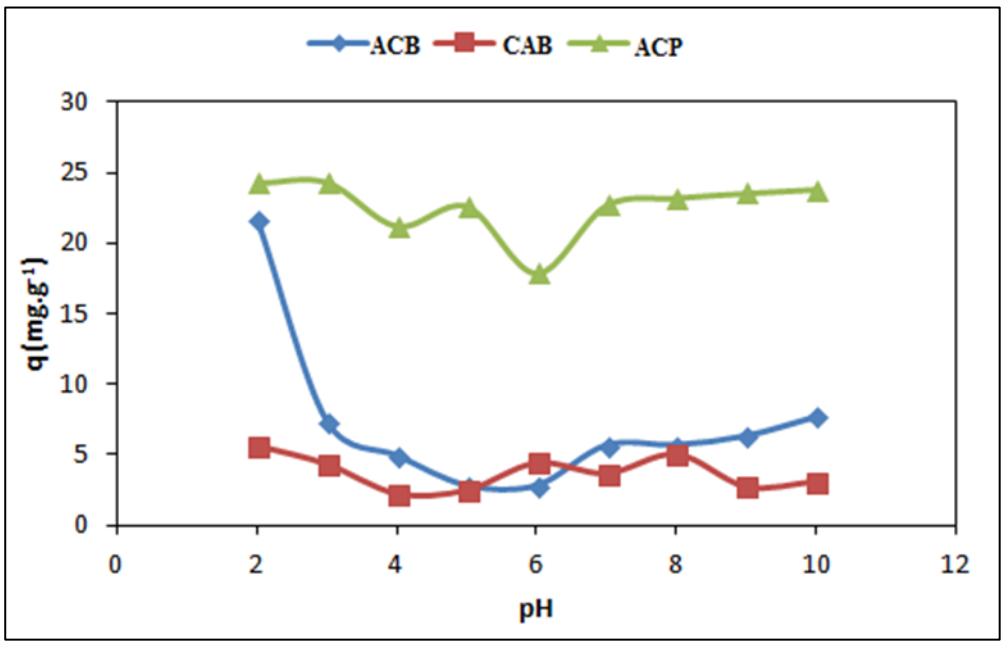

Source: Authors (2021)

3.4 Influence of adsorbent amount

The study of adsorbents mass was realized considering the results obtained in the solution pH experiment in order to determinate the sufficient mass to adsorb the maximum dye in the solution. Figure 6 displays the mass studies of the adsorbent.

As observed in Figure 6, the RGY removal increased together with the adsorbent concentration, reaching 92.21%, 20.84%, and 99.16% for the adsorbents ACB, CAB, and ACP, respectively, in 6 hours. This is justified by the superficial area increase resultant of the higher concentration of adsorbent and consequently, the rise of the number of sites (AHMED; THEYDAN, 2012). However, the amount of adsorbed dye by unit of adsorbent mass diminished with the increase of adsorbent

concentration. Hence, there is a reduction of the ratio adsorbate/adsorbent. According to Rodrigues *et al.* (2011), the decrease of the adsorption capacity is due to the overlap of sites because of the large amount of adsorbent particles, that results in the decrease of free area to adsorption.

Figure 6 - Study of the adsorbent concentration influence: (a) ACB; (b) CAB; (c) ACP of 0.06 g to 0.6g; C0 = 50 mg.L^{-1}, agitation speed = 300 rpm, t = 360 min, pH = 2

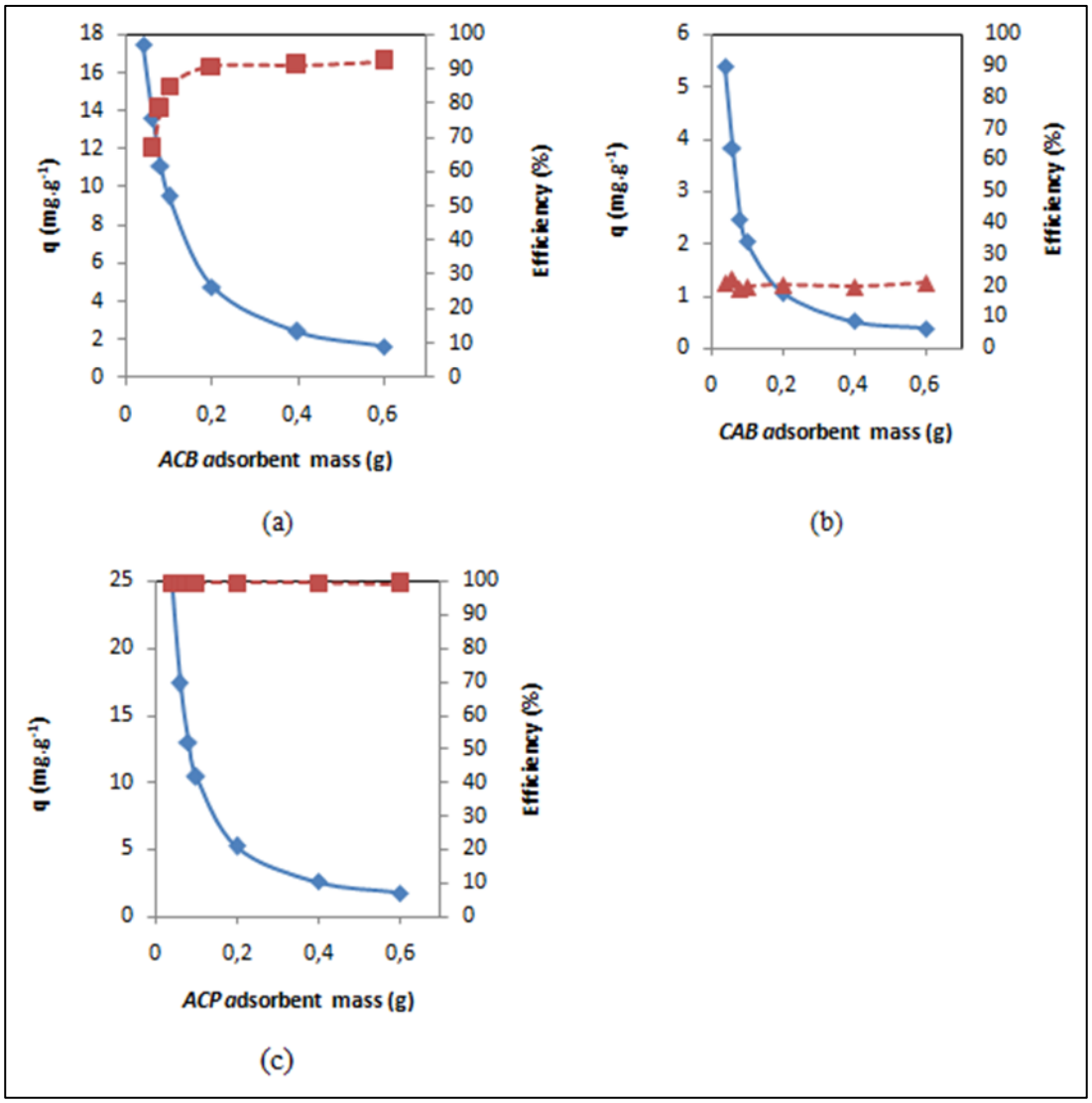

Source: Authors (2021)

The adsorption capacity decreased from 17.44 mg.g^{-1} (66.68% of removal) to 1.6116 mg.g^{-1} (92.68% of removal), for the raw acerola core bran (ACB). For the carbonized one, the reduction was from 5.39 mg.g^{-1} (20.61%) to 0.3635 mg.g^{-1}

(20.84%). For the charcoal activated before hand with H_2PO^4 (ACP), the decrease was from 25.798 $mg.g^{-1}$ (99.32% of removal) to 1.72 $mg.g^{-1}$ (99.16% of removal).

Evaluating the process through the exanimation of the Fig. 5, the adsorbents concentrations for ACB, CAB and ACP were 1.23 $g.L^{-1}$, 3.55 $g.L^{-1}$ and 0.2125 $g.L^{-1}$, respectively, corresponding to the curves intersection. These concentrations were used in the kinetic and equilibrium studies, aiming to find the best relation between removal percentage and adsorption capacity.

3.5 Kinetic and Adsorption Equilibrium Studies

The kinetics of the dye adsorption by the adsorbent material is fundamental to determine the best conditions for the large-scale process. From the mass studies results, kinetic studies were performed with different dye concentrations in order to determine the equilibrium time and the maximum adsorption capacity of the adsorbent.

The Figure 7 shows the adsorption capacity for different RGY concentrations (10 $mg.L^{-1}$ to 100 $mg.L^{-1}$), during 6 hours of treatment. It is perceived that the dye removal percentage for both adsorbents reduces while the initial concentration increases. This happens because of the adsorbent surface saturation in the process. Nonetheless, the increase of initial concentration leads to a rise of adsorption capacity.

The adsorbent CAB presented lesser adsorption capacity than ACB and FAP, as observed in Figure 7. Consequently, CAB performed less dye removal from the system. The dye removal percentage reached approximately 75% for ACB, 28% for CAB and 100% for ACP at the initial concentration of 60 $mg.L^{-1}$. Moreover, it was noticed that the maximum value of adsorption capacity occurred about 240 minutes. The experimental data is presented in Table S1 (Supplementary Material).

The kinetic studies were adjusted to the concentration of 60 $mg.L^{-1}$, in order to determine the mathematic model that best describes the curves. Figure 8

displays the curves of kinetic evolution of RGY adsorption on the adsorbents ACB, CAB and ACP with the adjustments of the non-linear kinetic models of pseudo-first order and pseudo-second order.

Figure 7 - Adsorption kinetics for different initial concentration of RGY dye: (a) ACB; (b) CAB; (c) ACP. Experimental conditions: Agitation speed = 300 rpm, t = 360 min, pH = 2

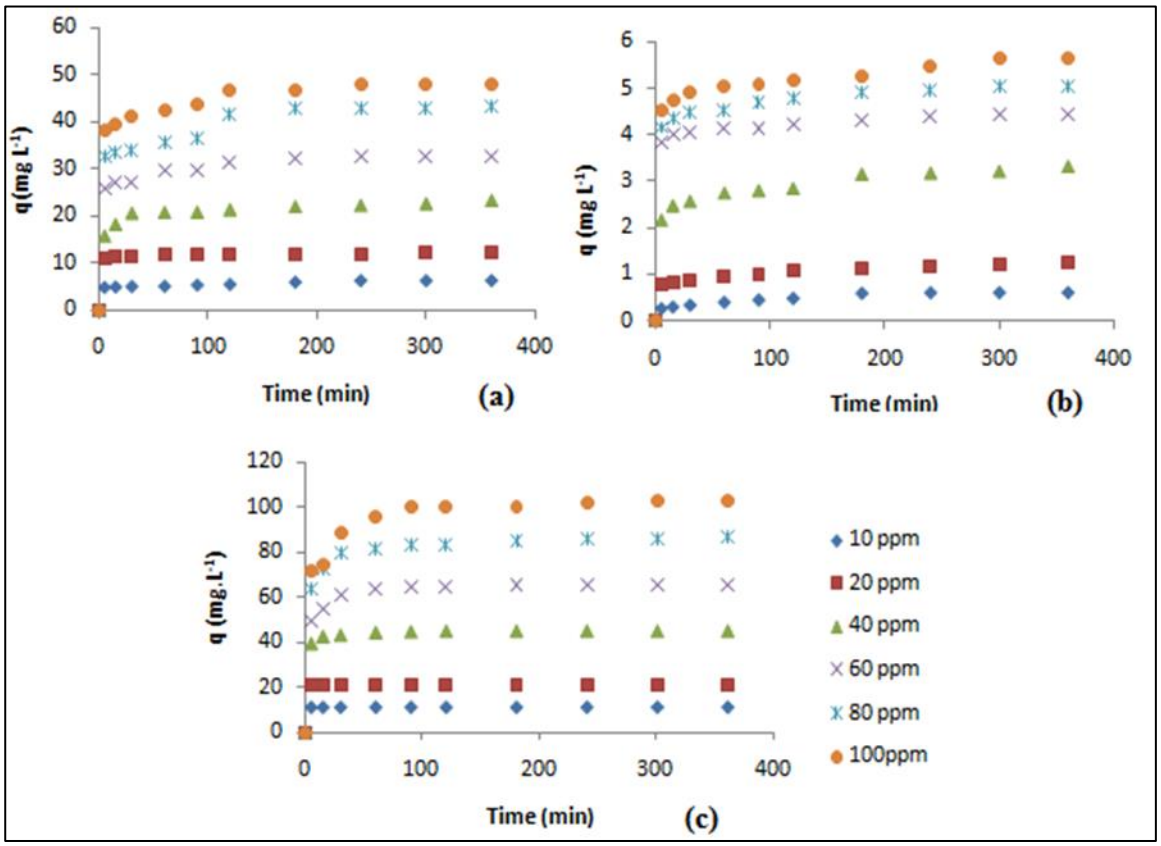

Source: Authors (2021)

There was a marked initial kinetic evolution, with major removal until 90 minutes for ACB and CAB and 60 minutes for ACP. Subsequently, a slow stage occurred with equilibrium at 240 minutes for the adsorbents ACB and CAB and 180 minutes for ACP. According to Schimmel et al. (2010), this behavior occurs because in the beginning of the adsorption process there is a large amount of empty sites for the adsorption. Along the time, this amount diminishes and repulsive forces of the adsorbed molecules begin to arise, what hinders the adsorption on the remaining sites.

The parameters of the kinetic models calculated for the adsorbents used in the RGY adsorption in aqueous solution are presented in Table 4.

Figure 8 - Adsorption kinetics with the non-linear model adjustments for (a) ACB ; (b) CAB; (c) ACP. Experimental conditions: C0= 60 mg.L^{-1}; agitation speed = 300 rpm, t= 360 min, pH=2

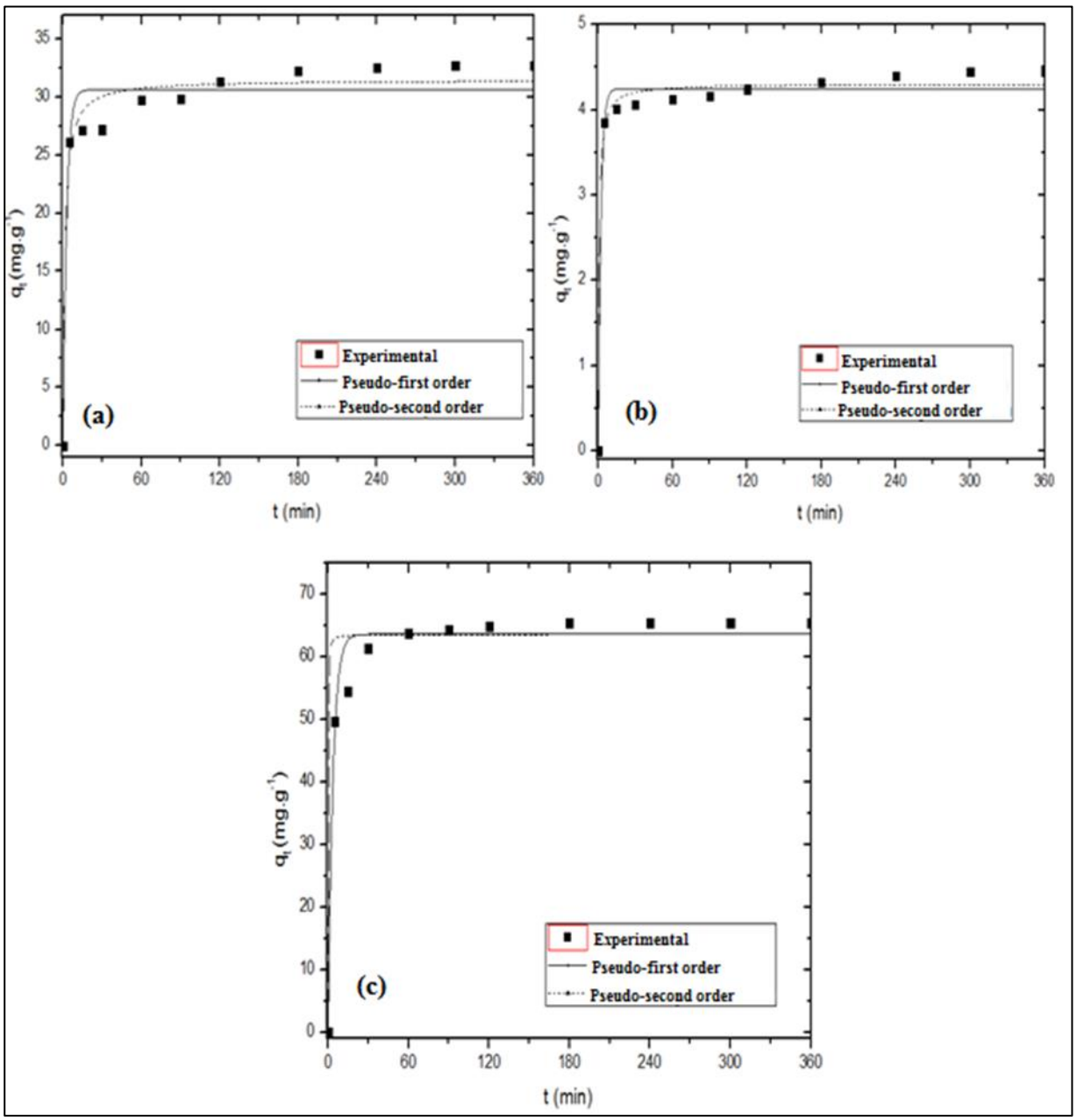

Source: Authors (2021)

Table 4 - Kinetic models parameters calculated for the adsorbents used in the RGY adsorption

Models	Parameters	ACB	CAB	ACP
Pseudo-first Order[1]	$q_{ecalc.}$(mg g^{-1})	30.627 ± 0.709	4.249 ± 0.052	63.651 ± 1.067
	k_1(min^{-1})	0.371 ± 0.092	0.470 ± 0.081	0.284 ± 0.042
	R^2	0.950	0.985	0.974
Pseudo-second Order[2]	$q_{ecalc.}$(mg g^{-1})	31.461 ± 0.609	4.307 ± 0.044	65.511 ± 0.572
	k_2 ($g.mg^{-1}.min^{-1}$)	0.02 ± 0.01	0.32 ± 0.09	0.008 ± 0.001
	R^2	0.972	0.992	0.994
Elovich[3]	a	5.256E5 ± 6.927E4	1.805 E10 ± 3.501E9	1.127 E6 ± 2.33E5
	b	0.562 ± 0.046	7.109 ± 0.478	0.274 ± 0.036
	R^2	0.996	0.999	0.989
F test	$F_{cal}^{1,2}$	1.82	1.74	4.72
	$F_{cal}^{1,3}$	11.84	15.52	2.46
	Fcal2,3	6.51	8.90	1.92
	Ftab	2.14	2.14	2.14

Source: Authors (2021)

In consonance with the F test, considering a confidence level of 95%, if Fcal < Ftab, does not exist significant difference among the models for the adjustment of experimental data. Regarding the adsorbent ACP, comparing the models of pseudo-first order and pseudo-second order, the last one obtained a better adjustment. However, despite the high R^2 value, Figure 8 shows that both models did not adjust to the data satisfactorily. Hence, according to Figure 7 and Table 4, the model that presented best adjustment for the adsorbents ACB and CAB, by the F test, was the Elovich model. This model can be fitted in general for slow and heterogeneous and localized layered adsorption processes. It is also an evidence that the adsorption is chemical type (ALJEBOREE *et al.* 2017; LARGITTE; PASQUIER, 2016). As observed in Figure 8, the systems do not reach equilibrium instantaneously, which may justify the adjustment in the proposed model.

The Figure 9 shows the adsorption isotherm with non-linear adjustments of the models of Langmuir, Freundlich and Fritz-Schlunder of the RGY solution using the adsorbents ACB, CAB and ACP. The experimental data is presented in Table S2 (Supplementary Material).

Figure 9 - Adsorption isotherms with non-linear adjustments of the kinetic models for (a)ACB; (b) CAB; (c) ACP

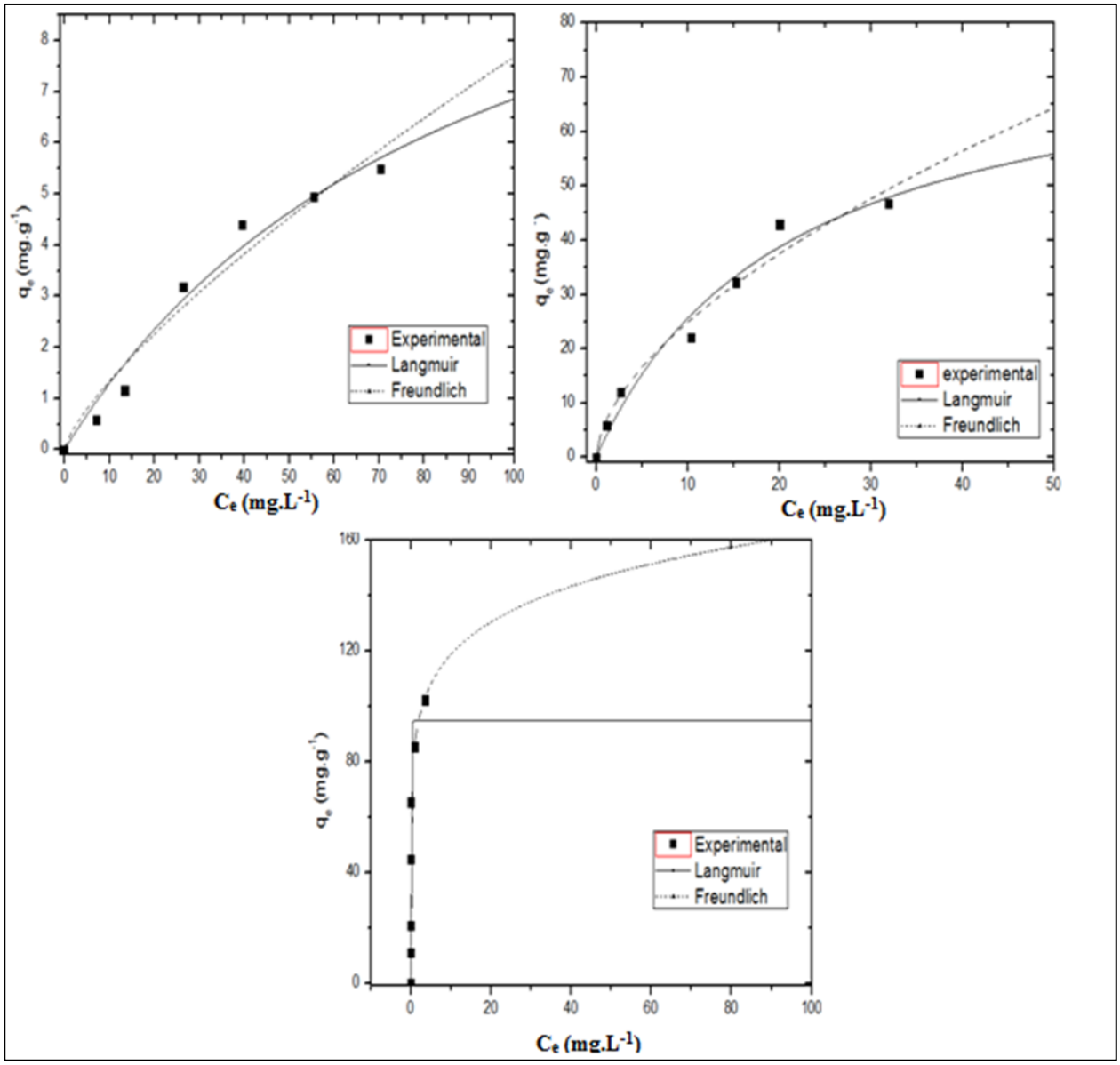

Source: Authors (2021)

The parameters of the kinetic models calculated for the prepared adsorbents in the dye RGY adsorption are displayed in Table 5. The parameters for the models

Langmuir, Freundlich and Fritz-Schlunder were obtained through the isotherms data in Figure 7 and by the equation 5 to 7, respectively. Considering the results of F test with confidence level of 95%, for the adsorbent ACB, the models Langmuir, Freundlich and Fritz-Schlunder demonstrated statistic equally, once every F_{calc} was lesser than F_{tab} (2.26). Related to CAB, the models Langmuir and pseudo-Freundlich were equal statistically, but Fritz-Schlunder presented the best adjustment. For ACP, Langmuir featured the best adjustment to experimental data.

Table 5 - Equilibrium models parameters calculated for the adsorbents used in the RGY adsorption

Models	Parameters	ACB	CAB	ACP
Langmuir[1]	q *max* ($mg.g^{-1}$)	78.715 ± 17.355	13.17 ± 4.513	94.996 ± 5.180
	K_L ($L.g^{-1}$)	0.048 ± 0.021	0.011 ± 0.006	434.520 ± 93.885
	R^2	0.953	0.958	0.958
Freundlich[2]	K_F ($L.g^{-1}$)	6.503 ± 1.586	0.232 ± 0.118	86.846 ± 10.135
	n	1.710 ± 0.236	1.316 ± 0.227	7.357 ± 2.007
	R^2	0.956	0.931	0.770
Fritz Schlunder[3]	K_{FS} ($L.g^{-1}$)	4.741 ± 2.015	0.010 ± 0.005	-
	a	1.467E-13 ± 7.676E-15	0.013 ± 0.002	-
	b_1	0.717 ± 0.172	1.959 ± 0.646	-
	b_2	9.413 ± 1.423	2.010 ± 0.306	-
	R^2	0.955	0.992	-
F test	$F_{cal}^{1,2}$	1.07	1.62	5.46
	$F_{cal}^{1,3}$	2.10	10.29	-
	$F_{cal}^{2,3}$	1.95	16.68	-
	F_{tab}	2.26	2.26	2.26

Source: Authors (2021)

The efficiency of the adsorbents utilized in this study was compared with results of other adsorbents reported in the literature in the phenolic compounds removal from aqueous solutions (Table 6).

Table 6 - Summary of the adsorption capacity values for the charcoals cited in the literature

Adsorbent	Co $mg.L^{-1}$	q_{max} $(mg.g^{-1})$	Reference
Charcoal from coffee waste activated with acetate	50	90.9	Lafi *et al.* 2018
Jute (*Corcholus olitorius*) stick charcoal	100	29.3	Chakraborty *et al.* 2020
Thuja orientales leaves charcoal activated with H_2SO_4	750	3.8	Arya *et al.* 2020
Charcoal from coconut shell nanofibers activated with polyvinyl alcohol	250	166.7	Widiyastuti *et al*. 2020
ACB	100	52.35	This work
CAB	100	16.4	This work
ACP	100	119	This work

Source: Authors (2021)

Through the analysis of the collected data, it is verified that the adsorbents raw, carbonized and activated have good efficiency related to the ones in the literature. The adsorption capacity of ACP was 56.00% and 86.26% greater than the ACB and CAB capacity respectively. As long as ACP is an agricultural waste, that is, a low cost resource, the raw material and the activated charcoal obtained from the

acerola core stand out as promising adsorbents for dye removal from industrial effluents.

4 CONCLUSÃO

The studied adsorbents presented good adsorption capability for the dye RGY in aqueous solution. It was verified that the dye solution at pH 2 enabled good adsorption. The activated charcoal (ACP) obtained from the acerola core presented greater adsorption capacity for the dye RGY removal in aqueous solution (119.4 $mg.g^{-1}$) than the other adsorbents. The kinetic study demonstrated that the best fit model for the RGY adsorption by the ACP adsorbent was Elovich's, while the equilibrium isotherms were best adjusted by the Fritz Schlunder model. The adsorbent ACB obtained adsorption capacity of 52.35 $mg.g^{-1}$, corresponding to 43.94% of the ACP efficiency and revealing a potential adsorbent for treatment of industrial waste contaminated by dyes, mainly due to its low cost of obtainment and production.

ACKNOWLEDGMENT

The authors are thankful for Clean Technology Laboratory (LATECLIM-UFPE) for characterization analysis.

REFERENCES

AHMED, M.; MASHKOOR, F.; NASAR, A. Development, characterization, and utilization of magnetized orange peel waste as a novel adsorbent for the confiscation of crystal violet dye from aqueous solution. **Groundwater for Sustainable Development**, v. 10, p. 1-10, 2020.

AHMED, M. J.; THEYDAN, S. K. Equilibrium isotherms, kinetics and thermodynamics studies of phenolic compounds adsorption on palm-tree fruit stones. **Ecotoxicology and Environmental Safety**, v.84, p. 39–45, 2012.

ALJEBOREE, A. M.; ALSHIRIFI, A. N.; ALKAIM, A. F. Kinetics and equilibrium study for the adsorption of textile dyes on coconut shell activated carbon. **Arabian Journal of Chemistry**, v. 10, p. S3381-S3393, 2017.

ANGIN, D. Utilization of activated carbon produced from fruit juice industry solid waste for the adsorption of Yellow 18 from aqueous solutions. **Bioresource Technology**, v.168, p.259–266, 2014.

ARAÚJO, K. S.; ANTONELLI, R.; GAYDECZKA, B.; GRANATO, A. C.; MALPASS, G. R. P. Processos oxidativos avançados: uma revisão de fundamentos e Efluentes, aplicações no tratamento de águas residuais urbanas e Industriais. **Revista Ambiente e Agua**, v.9, p.445–458, 2014.

ARYA, M. C.; BAFILA, P. S.; MISHRA, D.; NEGI, K.; KUMAR, R.; BUGHANI, A. Adsorptive removal of Remazol Brilliant Blue R dye from its aqueous solution by activated charcoal of Thuja orientalis leaves: an eco-friendly approach. **SN Aplplied Sciences**, v. 2, 265, 2020.

AVELAR, F. F.; BIANCHI, M. L.; GONÇALVES, M.; DA MOTA, E.G. The use of piassava fibers (Attalea funifera) in the preparation of activated carbon. **Bioresource Technology**, v.101, p.4639–4645, 2010.

AZIZ, A. R. A.; ASAITHAMBI, P.; DAUD, W. M. A. B. W. Combination of electrocoagulation with advanced oxidation processes for the treatment of distillery industrial effluent. **Process Safety and Environmental Protection**, Prot. v.99, p.227–235, 2016.

BARBOSA, A. A.; AQUINO, R. V. S.; OLIVEIRA, A. F. B.; DANTAS, R. F.; SILVA, J. P.; DUARTE, M. M. M. B., OTIDENE, R. S. R. 2019. Development of a new photocatalytic reactor built from recyclable material for the treatment of textile industry effluents. **Desalination and Water Treatment**, v.151, p. 82–92, 2019.

BAYOMIE, O. S.; KANDEEL, H.; SHOEIB, T.; YANG, H.; YOUSSEF, N.; EL-SAYED, M. M. H. Novel approach for effective removal of methylene blue dye from water using fava bean peel waste. **Scientific Reports**, v. 10, 7824, 2020.

BHATNAGAR, A.; SILLANPÄÄ, M. Utilization of agro-industrial and municipal waste materials as potential adsorbents for water treatment-A review. **Chemical Engineering Journal**, v.157, p.277–296, 2010.

BOUHADJRA, K.; LEMLIKCHI, W.; FERHATI, A.; MIGNARD, S. Enhancing removal efficiency of anionic dye (cibacron blue) using waste potato peels powder. **Scientific Reports**, v. 11, 2090, 2021.

CHAKMA, S.; DAS, L.; MOHOLKAR, V.S. Dye decolorization with hybrid advanced oxidation processes comprising sonolysis/Fenton-like/photo-ferrioxalate systems: A mechanistic investigation. **Separation and Purification Technology**, v.156, p.596–607, 2015.

CHAKRABORTY, T. K.; ISLAM, M. S.; KABIR, A. H. M. E.; GHOSH, G. C. Jute (Corcholus olitorius) stick charcoal as a low-cost adsorbent for the removal of methylene blue dye from aqueous solution. **SN applied Sciences**, v. 2, 765, 2020.

HASSAAN, M.A., EL NEMR, A., MADKOUR, F.F. Advanced oxidation processes of Mordant Violet 40 dye in freshwater and seawater. **Egyptian Journal of Aquatic Research**, v.43, p.1–9, 2017.

HOLKAR, C.R., JADHAV, A.J., PINJARI, D. V., MAHAMUNI, N.M., PANDIT, A.B. A critical review on textile wastewater treatments: Possible approaches. **Journal of Environmental Management**, v.182, p.351–366, 2016.

JARAMILLO-SIERRA, B.; MERCADO-CABRERA, A.; HERNÁNDEZ-ARIAS, A. N.; PEÑA-ERGUILUZ, R.; LÓPEZ-CALLEJAS, R.; RODRÍGUEZ-MÉNDEZ, B. G.; VALENCIA-ALVARADO, R. Methylene blue degradation assesment bo advanced oxidation methods. **Journal of Applied Research and Technology**, v.17, p.172-179, 2019.

LAFI, R.; MONTASSER, I.; HAFIANE, A. Adsorption of congo red dye from aqueous solutions by prepared activated carbon with oxygen-containing functional groups and its regeneration. **Adsorption Science and Technology**, v. 37, 160-181

LARGITTE, L.; PASQUIER, R. A review of the kinetics adsorption models and their application to the adsorption of lead by an activated carbon. **Chemical Engineering Research and Design**, v. 109, p. 495-504, 2016.

LI, H.; LIU, S.; ZHAO, J.; FENG, N. Removal of reactive dyes from wastewater assisted with kaolin clay by magnesium hydroxide coagulation process. **Colloids Surfaces A Physicochemical and Engineering Aspect**. v.494, p.222–227, 2016.

MONTGOMERY, D. C. **Introdução ao controle estatístico da qualidade (Introduction to statistical quality control)**. 4th ed. Rio de Janeiro: LTC, 2012.

REDDY, D. H. K.; RAMANA, D. K. V.; SESHAIAH, K.; REDDY, A. V. R. Biosorption of Ni(II) from aqueous phase by Moringa oleifera bark, a low cost biosorbent. **Desalination**, v.268, p.150–157, 2011.

RODRIGUES, L. A.; DA SILVA, M. L. C. P.; ALVAREZ-MENDES, M. O.; COUTINHO, A.; DOS, R.; THIM, G. P. Phenol removal from aqueous solution by activated carbon produced from avocado kernel seeds. **Chemical Engineering Journal**, v.174, p.49–57, 2011.

SÁNCHEZ-NAVA, D. M.; LÓPEZ-GONZÁLEZ, H.; OLGUÍN, M. T.; BULBULIAN, S. Nickel (II) sorption from aqueous media by Agave salmiana as biosorbent. **Journal of Applied Research and Technology**, v.17, p.186-194, 2019.

SCHIMMEL, D., FAGNANI, K.C., DOS SANTOS, J.B.O., BARROS, M.A.S.D., DA SILVA, E.A. Adsorption of turquoise blue qg reactive dye on commercial activated carbon in batch reactor:

Kinetic and equilibrium studies. **Brazilian Journal of Chemical Engineering**,. v.27, p.289–298, 2010.

SILVERSTEIN, R. M.; WEBSTER, F. X.; KIEMLE, D. J. **Identificaçãp Espectrométrica de Compostos Orgânicos (Spectrometric Identification of Organic Compounds).** 7th ed. Rio de Janeiro: LTC, 2006.

SOLOMONS, T. W. G.; FRYHLE, C.B. **Química Orgânica (Organic Chemistry).** 10th ed. Rio de Janeiro: LTC, 2012.

SOTO, M. L.; MOURE, A.; DOMÍNGUEZ, H.; PARAJÓ, J. C. Recovery, concentration and purification of phenolic compounds by adsorption: A review. **Journal of Food Engineering**, v.105, p.1–27, 2011.

TAGLIAFERRO, G. V.; PEREIRA, P. H. F.; RODRIGUES, L. Á.; PINTO DA SILVA, M. L. C. Adsorção de chumbo, cádmio e prata em óxido de nióbio (v) hidratado preparado pelo método da precipitaç ão em solução homogd̃nea. **Quimica Nova**, v.34, p. 101–105, 2011.

TOMUL, F.; ARSLAN, Y.; BAŞOĞLU, F. T.; BABUÇCUOĞLU, Y.; TRAN, H. N.Efficient removal of anti-inflammatory from solution by Fe-containing activated carbon: Adsorption kinetics, isotherms, and thermodynamics. **Journal of Environmental Management**, v.238, p.296–306, 2019.

TRAN, H. N.; CHAO, H. P. Adsorption and desorption of potentially toxic metals on modified biosorbents through new green grafting process. **Environmental Science and Pollution Research**, v.25, p.12808–12820, 2018.

VIOTTI, P. V.; MOREIRA, W. M.; SANTOS, O. A. A.; BERGAMASCO, R.; VIEIRA, A. M. S.; VIEIRA, M. F. (2019) Diclofenac removal from water by adsorption on Moringa oleifera pods and activated carbon: Mechanism, kinetic and equilibrium study. **Journal of Cleaner Production**, v.219, p.809–817, 2019.

WAWRZKIEWICZ, M.; WIŚNIEWSKA, M.; GUN'KO, V. M.; ZARKO, V. I. Adsorptive removal of acid, reactive and direct dyes from aqueous solutions and wastewater using mixed silica-alumina oxide. **Powder Technology**, v.278, p.306–315, 2015.

WIDIYASTUTI, W.; ROIS, M. F.; SUARI, N. M. I. P.; SETYAWAN, H. Activated carbon nanofibers derived from coconut shell charcoal for dye removal application. **Advanced Powder Technology**, v. 31, n. 8, p. 3267-3273, 2020.

ZHANG, B.; WU, Y.; CHA, L. Removal of methyl orange dye using activated biochar derived from pomelo peel wastes: performance, isotherm and kinetic studies. **Journal of Dispersion Science and Technology**, v. 41, n. 1, p. 125-136, 2020.

ZHAO, Y.; ZHU, L.; LI, W.; LIU, J.; LIU, X.; HUANG, K. Insights into enhanced adsorptive removal of rhodamine B by different chemically modified garlic peels: Comparison, kinetics, isotherms, thermodynamics and mechanism. **Journal of Molecular Liquids**, v. 293, p. 1-10, 2019.

Authorship contributions

1- Ada Azevedo Barbosay
Chemical Engineer, PhD in Chemical Engineering
http://orcid.org/0000-0002-9169-0574 - adabarbosa@hotmail.com
Contributions: Conceptualization | Data Curation | Formal Analysis | Investigation| Methodology | Validation | Visualization | Writing – original draft | Writing – review & editing

2- Marina Gomes Silva
Chemical Engineer, Master's student in chemical engineering
https://orcid.org/0000-0002-8835-7308 - marina.g.silva@hotmail.com
Contributions: Data Curation | Methodology | Validation | Visualization | Writing – original draft

3- Ingrid Larissa da Silva Santana
Chemical Engineer, Master's student in chemical engineering
https://orcid.org/0000-0001-8545-6637 - ingrid---larissa@hotmail.com
Contributions: Data Curation | Methodology | Validation | Visualization | Writing – original draft

4- Ramon Vinícius Santos de Aquino
Chemical Engineer, Master's student in chemical engineering
https://orcid.org/0000-0003-4784-3251 - viniciusramon59@gmail.com
Contributions: Data Curation | Methodology | Validation | Visualization | Writing – original draft | Writing – review & editing

5- Naiana Santos da Cruz Santana Neves
Chemical Engineer, PhD student in chemical engineering
https://orcid.org/0000-0001-8494-8058 - naiana.santana@hotmail.com
Contributions: Data Curation | Methodology | Validation | Visualization | Writing – original draft | Writing – review & editing

6- Isis Henriqueta dos Reis Ferreira
Chemical Engineer, Master's student in chemical engineering
https://orcid.org/0000-0002-0925-3878 - isisfreis@yahoo.com
Contributions: Writing – original draft | Writing – review & editing

7- Otidene Rossiter Sá da Rocha
Chemical Engineer, PhD in Chemical Engineering
https://orcid.org/0000-0001-5216-1752 - otidene@hotmail.com
Contributions: Conceptualization | Investigation | Project Administration | Resources | Supervision | Writing – review & editing

How to quote this article

Simioni, C.F.; Almeida, F.T.; Zolin, C.A.; Uliana, E.M.; Souza, A.P.; Marques, A. Solid discharge in a microbasin of the Amazon region. **Ciência e Natura**, Santa Maria, v. 43, e73, p. 1-28, 2021. DOI 10.5902/2179460X64223. Available from: https://doi.org/10.5902/2179460X64223.

ANEXO

Table S1 - Experimental data for kinetic study